Enhancing wheat crop physiology monitoring through spectroscopic analysis of stomatal conductance dynamics

Cheng, K.H.; Sun, Z.; Zhong, W.; Wang, Z.; Visser, M.D.; Liu, S.; ... ; Wu, J.

Remote Sensing of Environment 312 (2024) 114325

Contents lists available at ScienceDirect

Remote Sensing of Environment

journal homepage: www.elsevier.com/locate/rse

Enhancing wheat crop physiology monitoring through spectroscopic analysis of stomatal conductance dynamics

K.H. Cheng [a,b], Zhuangzhuang Sun [c,*], Wanlu Zhong [a], Zhihui Wang [d], Marco Visser [e], Shuwen Liu [a], Zhengbing Yan [f], Yingyi Zhao [a], Ruinan Zhang [c], Jingrong Zang [c], Shichao Jin [c], Jin Wu [a,g,*]

[a] Research Area of Ecology and Biodiversity, School of Biological Sciences, The University of Hong Kong, Pokfulam, Hong Kong, China
[b] School of Life Sciences, The Chinese University of Hong Kong, Shatin, Hong Kong, China
[c] Plant Phenomics Research Centre, Academy for Advanced Interdisciplinary Studies, Collaborative Innovation Centre for Modern Crop Production Co-Sponsored by Province and Ministry, College of Agriculture, Nanjing Agricultural University, Nanjing, China
[d] Guangdong Provincial Key Laboratory of Remote Sensing and Geographical Information System, Guangdong Open Laboratory of Geospatial Information Technology and Application, Guangzhou Institute of Geography, Guangdong Academy of Sciences, Guangzhou, China
[e] Institute of Environmental Sciences, Leiden University, Einsteinweg 2, 2333 CC Leiden, the Netherlands
[f] State Key Laboratory of Vegetation and Environmental Change, Institute of Botany, Chinese Academy of Sciences, Xiangshan, Beijing, China
[g] Institute for Climate and Carbon Neutrality, The University of Hong Kong, Pokfulam, Hong Kong, China

ARTICLE INFO

Edited by Jing M. Chen

Keywords:
Crop physiology
Stomatal conductance
Stomatal anatomical/behavioral traits
Spectroscopy
Spectra-trait associations
Precision agriculture

ABSTRACT

Monitoring *in-vivo* stomatal conductance (g_s) dynamics is essential for predicting crop water usage and yield sensitivity in response to climate change. Leaf and canopy spectroscopy offer a non-destructive method for g_s monitoring; however, the underlying mechanisms connecting leaf spectra with stomatal anatomical and behavioral traits, and their subsequent impacts on g_s, remain underexplored. In this study, we conducted a wheat field trial, collecting comprehensive measurements of stomatal anatomical (*i.e.*, size, density) and behavioral (*i.e.*, opening ratio, pore area) traits by a customized, high-resolution microscope, leaf spectra *via* a handheld spectroradiometer, and g_s *via* a handheld AP4 Leaf Porometer across various genotypes, nitrogen treatments, growth stages, and diurnal environments. We observed substantial g_s variability, with stomatal anatomical and behavioral traits jointly accounting for 79% of this variability. We further examined the relationship between leaf spectra and stomatal traits/conductance using a partial least square regression (PLSR) model and discovered that a single PLSR spectral model accurately predicted the variability of each of these traits and g_s across our datasets. Furthermore, we demonstrated a strong correspondence between spectral variations resulting from g_s and spectral alternation induced by stomatal anatomical and behavioral traits. By analyzing the diurnal association between spectral and g_s variability, we revealed important biophysical mechanisms underlying relationships among spectra, stomatal anatomical and behavioral traits, and g_s. Collectively, our findings highlight the potential of leaf spectroscopy in advancing crop physiology monitoring, contributing to enhanced food security and sustainability.

1. Introduction

The escalating global temperatures and increasing frequency of droughts have heightened concerns over diminishing crop productivity and food security. This has underscored the need for innovative approaches to enhance crop yields and ensure food sustainability (Dhankher and Foyer, 2018; Haile, 2005; Wheeler and Von Braun, 2013). Stomatal regulation, as indicated by stomatal conductance (g_s), plays a vital role in balancing plant photosynthetic CO_2 uptake and water loss. This significantly impacts photosynthesis and crop water use throughout the growing season, ultimately affecting overall crop yield and productivity (Hetherington and Woodward, 2003; McAusland et al.,

* Corresponding authors at: Research Area of Ecology and Biodiversity, School of Biological Sciences, The University of Hong Kong, Pokfulam, Hong Kong, China; Plant Phenomics Research Centre, Academy for Advanced Interdisciplinary Studies, Collaborative Innovation Centre for Modern Crop Production Co-Sponsored by Province and Ministry, College of Agriculture, Nanjing Agricultural University, Nanjing, China.
E-mail addresses: 2020201018@stu.njau.edu.cn (Z. Sun), jinwu@hku.hk (J. Wu).

https://doi.org/10.1016/j.rse.2024.114325
Received 16 October 2023; Received in revised form 28 March 2024; Accepted 20 July 2024
Available online 24 July 2024

2016; Wong et al., 1979). Therefore, an improved understanding and monitoring of g_s are critical for developing innovative approaches to boost crop productivity in the face of climate change.

Research from field-, experimental-, and modeling-based studies have increasingly revealed the highly dynamic nature of g_s over diurnal and seasonal time scales (Franks and Beerling, 2009; McAusland et al., 2016; Faralli et al., 2019). This dynamism is influenced by a combination of intrinsic factors associated with stomatal anatomical traits and plant water use strategy, as well as external environmental factors that interact with stomatal behavioral traits (*i.e.*, stomatal opening and closure). The interplay between these factors ultimately governs the modulation of *in-vivo* g_s dynamics (Dow et al., 2014; Faralli et al., 2022; McAusland et al., 2016). For example, stomatal anatomical traits, such as stomatal size and density, significantly impact g_s magnitude and determine the theoretical maximum g_s (Franks and Beerling, 2009; Galmés et al., 2013). These traits are also closely associated with different plant species, genotypes, and growth stages, illustrating varying water use efficiencies and photosynthetic capacities (Fig. 1a, Shabala et al., 2013; Faralli et al., 2019). Additionally, stomatal behavioral traits (*i.e.*, the percentage of stomata with opening among all stomata detected in a given leaf surface area) respond to ambient environment conditions, with factors such as light, temperature, humidity and other stressors (*i.e.*, water deficit or nutrient limits) directly or indirectly influencing these behavioral traits, thereby affecting gas exchange and plant water use (Dow et al., 2014; Faralli et al., 2022; Franks and Beerling, 2009; Galmés et al., 2013; McAusland et al., 2016). While mathematical and computational models have simulated these relationships between g_s and environmental variables (Buckley, 2017; Medlyn et al., 2011; Wu et al., 2020), our understanding of how stomatal anatomical and behavioral traits interactively determine *in-vivo* g_s dynamics in response to ambient environmental conditions remains limited.

This limitation is fundamentally attributed to the difficulty in *in-vivo* measurements of g_s and stomatal behavioral traits. Conventional methods, such as leaf-level g_s monitoring using a porometer or gas exchange system (Dayer et al., 2020), are time-consuming, labor-intensive, and have limited throughput capability (Lin et al., 2015; Wang et al., 2022; Wu et al., 2020), rendering them ill-suited for rapid and large-scale monitoring. Various methods, such as the integration of eddy

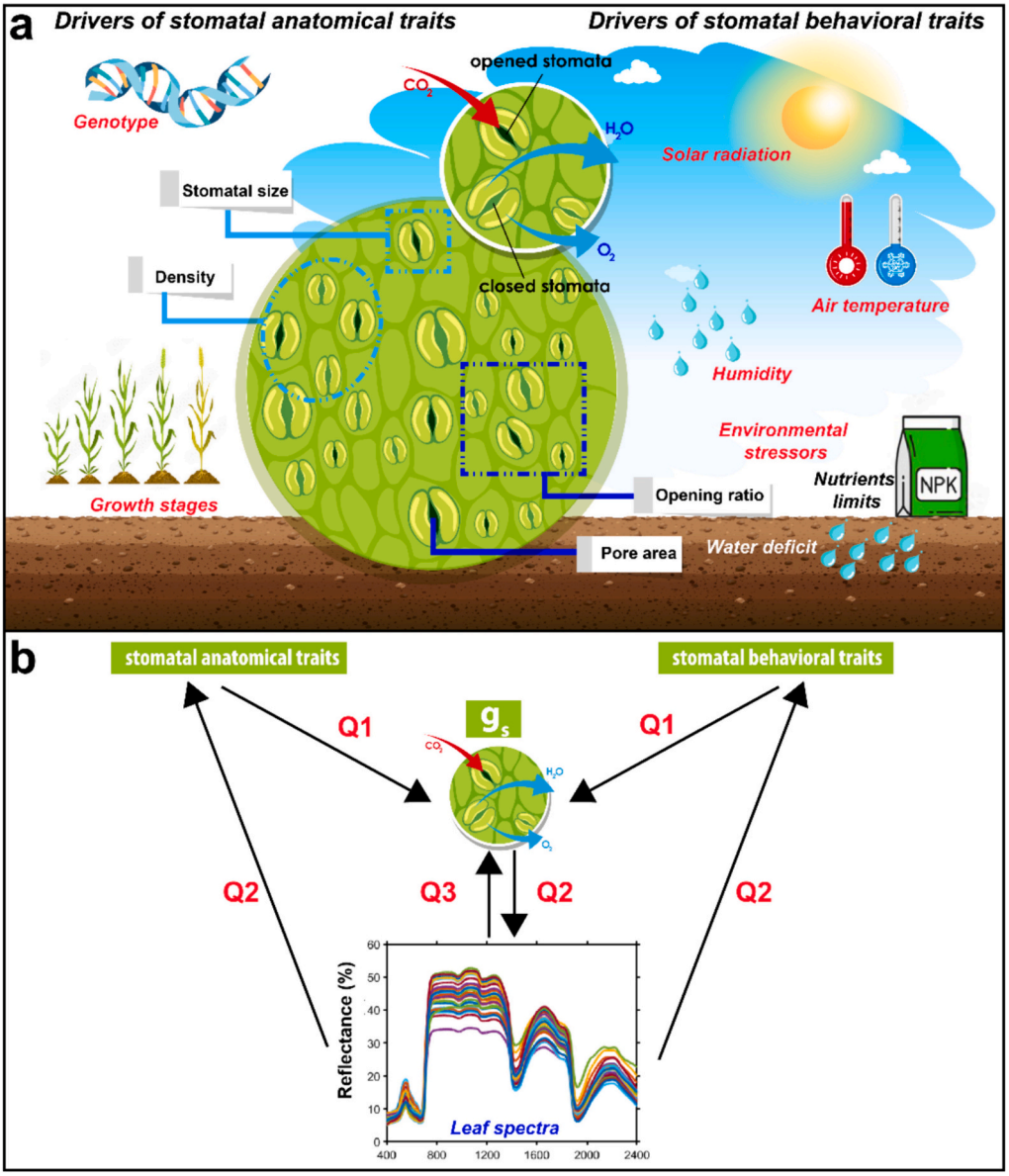

Fig. 1. (a) Drivers of stomatal anatomical and behavioral traits; (b) conceptual research questions of the role for leaf spectra in predicting stomatal conductance (g_s), stomatal anatomical and behavioral traits, and their underlying links.

covariance flux measurements (Jin et al., 2022; Perez-Priego et al., 2018) or satellite data (Ding et al., 2023) with process-based models, have been increasingly used to infer g_s of the forest canopy. For example, Perez-Priego et al. (2018) calculated the canopy g_s from eddy covariance fluxes using a combination of physiological and micrometeorological approaches. However, it is still difficult to monitor g_s at the organ level (Medlyn et al., 2017). Moreover, stomatal behavioral traits are highly dynamic, making them challenging to monitor using conventional destructive sampling methods (*i.e.*, nail polish method (Zelitch, 1961)). Consequently, there is an urgent need for alternative methods that enable rapid (and potentially scalable), non-destructive monitoring of fine-scale (*i.e.*, diurnal) dynamics in both g_s and stomatal behaviors.

Recent advances in *in-vivo* microscopy imaging techniques and vegetation spectroscopy offer promising solutions for monitoring stomatal anatomical traits and *in-vivo* stomatal behavioral traits. Micro-imaging techniques provide an unpresented opportunity to observe these traits in real-time. For example, Sun et al. (2023) combined a portable micro-imaging system with an automatic imaging acquisition system and a deep learning technique to monitor stomata in real-time, revealing highly-dynamic stomatal behaviors even within a single day. Yang et al. (2023) showed that drought priming led to faster stomatal closure under drought stress through *in-situ* monitoring of dynamic stomatal behaviors in wheat. Likewise, Liang et al. (2022) investigated dynamic stomatal changes in maize under drought and re-watering conditions using micro-imaging techniques. These findings highlight the effectiveness of micro-imaging techniques for monitoring *in-vivo* stomatal behaviors and their dynamic nature influenced by environmental factors.

Furthermore, recent advance in vegetation spectroscopy studies may provide promising alternatives for g_s and stomatal anatomical/behavioral traits monitoring. Plant and leaf hyperspectral data can be viewed as a combination of optical characteristics associated with various leaf morphological and biochemical attributes, connected through electronic and vibrational absorption processes (Curran, 1989; Kokaly et al., 2009; Schweiger et al., 2018). For example, previous studies documented the sensitive spectral domains for leaf xanthophyll pigment (400–531 nm) and leaf water content (503–632 nm, near 1450 nm, and 1950–1980 nm,) (Curran, 1989; Datt, 1999; El-Hendawy et al., 2019; Sims and Gamon, 2002). And typical spectra-derived metrics for leaf xanthophyll pigment and leaf water content have been widely used. Gamon et al. (1992) proposed the photochemical reflectance index (PRI_{570}) to infer xanthophyll pigment, which could co-vary with *in-vivo* plant physiological activities (Gamon and Surfus, 1999; Ollinger, 2011), and Zarco-Tejada et al. (2013) recommended the normalized PRI (PRI_{norm}) for wider application. Additionally, indices related to leaf water content, which often co-vary with *in-vivo* stomatal dynamics (Brodribb and McAdam, 2017; Buckley et al., 2011), such as leaf water index (*LWI*, Seelig et al., 2009) and moisture stress index (*MSI*, Hunt Jr and Rock, 1989) MSI $= R_{1600}/R_{820}$, have been previously developed and validated using leaf hyperspectral data. Equations of these metrics are summarized in Table S1. Recent studies demonstrate the capability of using full leaf reflectance spectra to infer a broad suite of leaf traits, including leaf morphological (*i.e.*, leaf mass per area), biochemical (*i.e.*, water, chlorophyll, nitrogen, and phosphorous) and physiological traits (*i.e.*, $V_{c,max25}$ and J_{max25}) with a high accuracy (Meacham-Hensold et al., 2020; Serbin et al., 2015; Yan et al., 2021). Thus, leaf and canopy hyperspectral data offer accurate, generalizable, and high-throughput tools for multi-dimensional leaf trait characterizations (Fu et al., 2020; Liu et al., 2023).

Importantly, recent studies conducted in various agroecosystems and natural ecosystems have demonstrated the immense potential of using leaf spectroscopy as alternative, non-destructive means for sensing leaf photosynthesis rates, respiration rates and g_s (Coast et al., 2019; O'Leary et al., 2023; Shahrimie et al., 2022; Sobejano-Paz et al., 2020; Vitrack-Tamam et al., 2020; Zhang et al., 2022). Although these studies primarily relied on data-driven approaches, they proved that combining spectroscopy with machine learning can serve as a promising alternative for advancing the monitoring of plant photosynthesis, respiration, and g_s at finer time scales. However, the mechanisms underlying the spectroscopy of these fine-scale dynamics of plant physiological rate dynamics (*i.e.*, g_s and stomatal anatomical/behavioral traits) remain underexplored. Considering that g_s is impacted by both stomatal anatomical and behavioral characteristics, we hypothesize that if leaf spectra co-varies with temporal variation in stomatal anatomical and behavioral, it is plausible that there are causal connections that ultimately link to spectra to the dynamics of g_s. Moreover, since g_s and stomatal behavioral traits are known to vary significantly across diurnal environments, examining their diurnal relationships through leaf reflectance spectra could provide a crucial threshold test to determine if the observed linkages are genuine or merely coincidental. Investigating the diurnal variations in leaf reflectance spectra for the same leaf over time, and the diurnal association of g_s and stomatal behavioral traits with spectra-derived leaf xanthophyll pigment (*i.e.*, PRI_{norm}) and water content (*i.e.*, *LWI*) may help reveal the potential mechanism underlying the relationship between leaf spectra, g_s, and stomatal traits. Despite its simplicity, this threshold test remains largely unexplored due to the challenges in collecting all these paired data in the field.

This research aims to enhance our understanding of the biological processes regulating *in-vivo* g_s dynamics and investigate the models and mechanisms underlying the spectroscopy of diurnal g_s. To accomplish this, we conducted a wheat field trial to collect comprehensive data on stomatal anatomical and behavioral traits, g_s, and leaf spectra. Notably, we employed state-of-the-art microscopy imaging and deep learning techniques to enable *in-vivo* monitoring of both stomatal anatomical and behavioral traits (Sun et al., 2023). Specifically, we address three questions (Fig. 1b): (1) How do stomatal anatomical and behavioral traits regulate *in-vivo* g_s dynamics? (2) Are spectral variations due to g_s linked to reflectance changes that strongly correspond with spectral alternation induced by associated stomatal traits? and (3) What are potential underlying biochemical connections between stomatal traits and g_s, and leaf spectra? Addressing these questions would ultimately contribute to improved g_s monitoring and elucidate the biological mechanisms underlying spectral sensing of g_s.

2. Materials and methods

2.1. Study site and crop materials

This study was carried out at the Baima Experimental Station (119°18′71″E, 31°62′00″N) of Nanjing Agricultural University, China (Fig. 2a) from November 2022 to May 2023. The region features a subtropical monsoon climate, with an average annual precipitation of 1037 mm and an annual mean temperature of 15.5 °C. The research station covers a total planting area of 3750 m^2, comprising 1260 plots. These plots were cultivated with 210 Chinese winter wheat genotypes, subjected to two nitrogen fertilization treatments (0 and 240 kg/ha), and replicated three times following a split-plot design. Notably, all of our wheat plots consistently underwent pest control, weeding, and irrigation, in addition to following general field management practices. Each plot has a grid size of 1.25 m × 1.5 m, with 0.5 m spacing between plots and 0.45 m between rows. The germplasm density was maintained at 300 seeds/m^2. The diverse stomatal traits and g_s values observed resulted from variations in genotypes, nitrogen treatments, and growth stages, providing a comprehensive range for subsequent analyses.

2.2. Field measurements

In-vivo measurements of leaf g_s, microscopy imaging, and leaf spectra were conducted in April–May 2023 (Fig. 2b) on >70 Chinese winter wheat genotypes across six growth stages (tillering, stem elongation, booting, heading, flowering and ripening). To address the first question while considering the highly dynamic variations of leaf g_s and stomatal

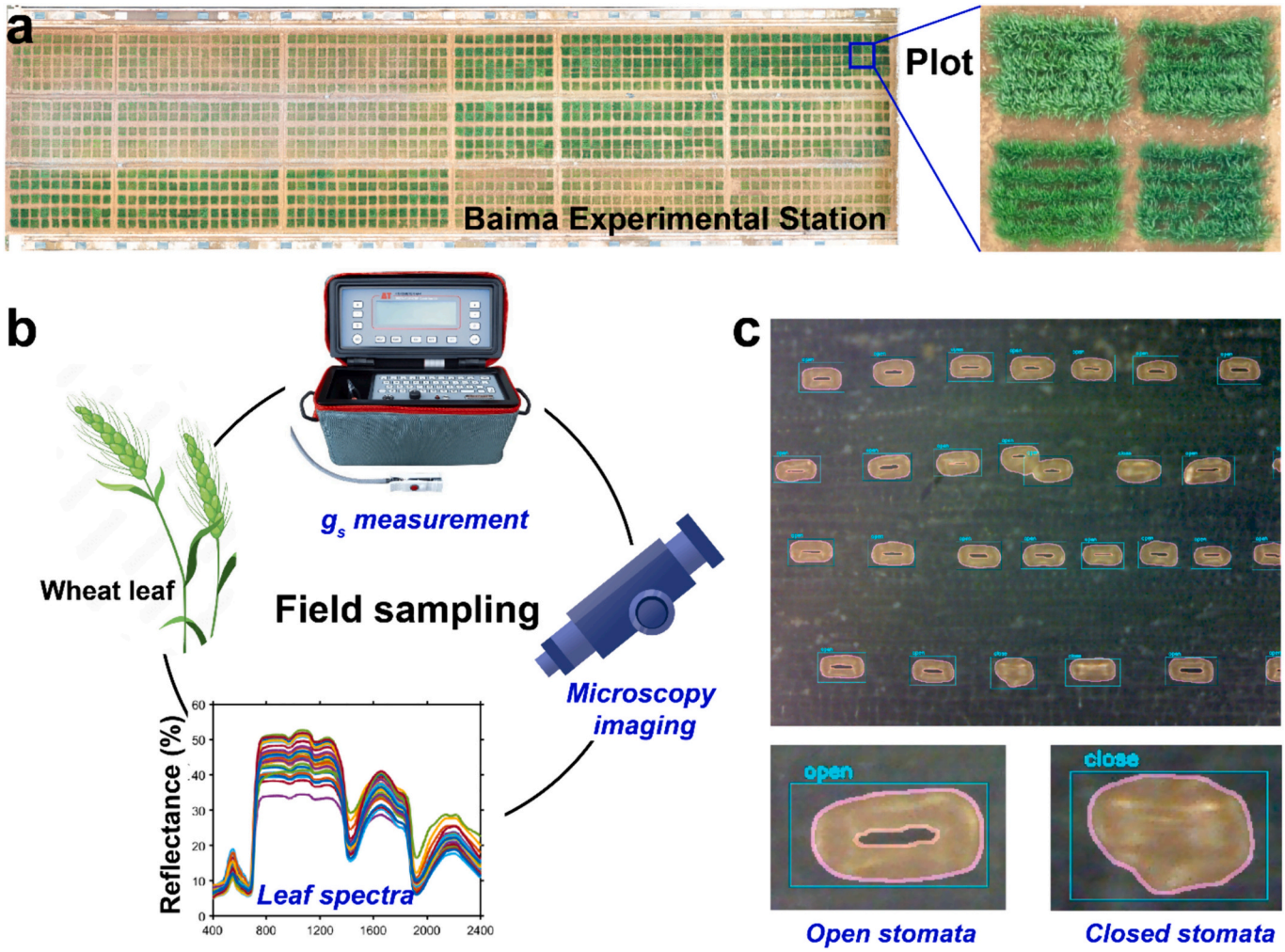

Fig. 2. (a) Study site: Baima Experimental Station of Nanjing Agricultural University, China; (b) field *in-vivo* sampling workflow; and (c) demonstrations of microscopy images for stomata. g_s denotes stomatal conductance.

behavioral traits, we randomly selected fully expanded wheat leaves and measured leaf g_s and microscopy images without spectra data, minimizing the time gap between measurements. A total of 516 samples were collected. For the second question, we gathered an additional 361 samples with leaf spectra and microscopy image data. Notably, 56 out of 361 samples also included leaf g_s data for exploring the third question. These 56 paired data (leaf g_s, spectra, and microscopy images) were collected from seven sampling revisits of eight identical wheat leaves during a day-long sampling campaign, allowing us to isolate the effects of genotype, growth stage, and nitrogen fertilization treatments on leaf spectra as much as possible. Specifically, we examined five representative wheat genotypes, with three genotypes subjected to two nitrogen fertilization treatments, and the remaining two genotypes subjected to one nitrogen fertilization treatment. The sampling campaign occurred from 7 am to 6 pm, with a 1.5-h time window for each revisit. Fig. S1 summarizes the data collection and usage. During field sampling, we carefully collected leaf g_s, spectra and microscopy images from the same spot of the leaf to maintain consistency and accuracy, minimizing potential variabilities or bias that might arise if sampling different spots on the wheat leaf. We also performed 20% duplicate samples to validate field data.

2.2.1. Leaf g_s measurement

We measured leaf *gs* using a handheld AP4 Leaf Porometer (Delta-T Devices, Burwell, Cambridge, UK), performing three replicates per leaf sample. To obtain a wide range of reliable g_s values within the AP4 specifications, we followed the approach of Mantzoukas et al. (2015) by measuring resistance and calculating its reciprocal as g_s. Consequently, leaf g_s is expressed in mm s^{-1} and includes records of time, light intensity, and temperature. The AP4 Leaf Porometer has a reading range of 0.2–40 s cm^{-1} for resistance, a resolution of 0.01–0.1 s cm^{-1}, and an accuracy of ±10% for of 0.5–40 s cm^{-1} and ± 0.2 s cm^{-1} for 0.2–0.5 s cm^{-1} (https://delta-t.co.uk/product/ap4/#specification).

2.2.2. Microscope imaging

We collected stomatal images using an *in-vivo* stomatal behavior observation system (HT-WC-USB600–1; Huitong Crop Phenomics Co., Ltd.; China), which enables dynamic monitoring of stomatal anatomical and behavioral traits using a portable microscope. The portable microscope was placed 1 cm above the leaves by a soft leaf chamber, ensuring that the ambient environment and plant physiology remained undisturbed. We captured adaxial leaf images at 600× magnification and saved them in JPG format with a resolution of 1200 × 1600 pixels and a spatial resolution of 0.61 μm/pixel. Subsequently, we employed the image processing method by Sun et al. (2023) to extract four widely-used and representative stomatal metrics: anatomical traits (size, density) and behavioral traits (opening ratio, pore area) (Franks and Beerling, 2009; Mott and Buckley, 1998; Xie et al., 2022). Specifically, stomatal density (pore mm^{-2}) is calculated as the total stomatal number divided by the entire image area; stomatal size (μm^2) refers to the mean

stomatal size, determined as the total stomatal area divided by the stomatal number; open ratio (dimensionless) refers to the proportion of open stomata relative to the total stomatal count; and pore area (μm^2) denotes the mean effective pore area, calculated as the stomatal pore area divided by the open stomata count.

The image processing pipeline consists of two modules: detection and segmentation. The first module employs a high-detection-efficient lightweight object detector (YOLOv3-tiny, a one-stage object detection algorithm) (Gong et al., 2020) for effective identification of stomatal numbers, and opening/closing statuses. The second module involves a segmentation process that converts stomatal image into binary images, including masks of each stoma, from which stomatal metrics can be obtained through conventional morphological analysis. The quantitative assessment on the retrieved stomatal traits and behaviors has been rigorously evaluated previously with high accuracy, and details of this method can be found in Sun et al. (2023).

2.2.3. Leaf spectra

We measured leaf reflectance using a field-portable Spectra Vista Corporation (SVC, Poughkeepsie, NY, USA) HR-1024i spectroradiometer equipped with a Leaf-Clip Reflectance-Probe (LC-RP-Pro) foreoptic. The spectra spanned a range of 350–2500 nm (with a full-width half maximum (FWHM) $\leq$ 3.3 nm at 700 nm, $\leq$ 9.5 nm at 1500 nm, and $\leq$ 6.5 nm at 2100 nm) and were linearly interpolated into 1 nm intervals for analysis, following Yan et al. (2021). Spectral regions below 400 nm and above 2400 nm with higher noise levels were excluded from the analysis (Schweiger et al., 2018). A calibrated internal light source and a 99% reflective Spectralon white panel were utilized to minimize ambient light effects and ensure consistent measurements, as recommended by Yan et al. (2021). This allows for data collection across the diurnal cycle independent of sunlight. Consequently, our approach, compared to traditional methods relying on tower- or tripod-mounted spectroradiometers, is insensitive to ambient light conditions and diurnal variations in sun angle. In the meanwhile, the spectrometer was set to a 1-s integration time to prevent heat-induced data quality issues (Serbin et al., 2019), and the spectra were corrected for discontinuities using vendor-provided software (Yan et al., 2021). Four repetitions were measured for each sample, and the averaged spectra were used.

2.3. Data analysis

Our objective was to investigate the relationship between leaf spectra, stomatal anatomical and behavioral traits (size, density, opening ratio, and pore area), and g_s. First, we examined the relationship between stomatal traits (both anatomical and behavioral) and g_s. Next, we investigated the associations between these traits and leaf spectra. Finally, we explored the potential connections between g_s and leaf spectra.

2.3.1. Exploring the associations between stomatal anatomical/behavioral traits and g_s

We performed two analyses to assess the associations between stomatal anatomical and behavioral traits and g_s: (1) ordinary least squares regression to examine the relationships between g_s and individual stomatal metrics, and (2) boosted regression trees (BRT) regression to explore the joint regulation of four stomatal metrics and rank their independent importance on g_s. Notably, BRT, a non-parametric ensemble method, offers several advantages, such as flexibility in handling different data types, the ability to identify non-linear relationships and interactions between variables, high interpretability of feature importance, and robustness to outliers and missing values (Elith et al., 2008; Sporbert et al., 2022), and thus was used in this study. To assess the general association between g_s and stomatal metrics, we considered g_s as the dependent variable and four stomatal metrics as explanatory variables. The BRT modeling approach was adapted from Sporbert et al. (2022) and implemented using the R package 'GBM' v.2.1.8.1 (Greenwell et al., 2019), with a Gaussian error distribution, bag fraction of 0.5, tree complexity of 1, and a learning rate of 0.01. To ensure the rigor of the BRT modeling, the dataset ($n = 516$) was randomly stratified into an 80% training subset and a 20% independent validation subset, following Wu et al. (2019). This random stratification would ensure representation of stomatal metrics and g_s in both training and validation subsets. For the training subset, during the model development, we used tenfold cross-validation to optimize the number of trees while avoiding overfitting. The performance of the optimized BRT model was subsequently assessed using the validation subset, with two evaluation metrics: the coefficients of determination (R^2) and root mean squared error (RMSE). Decision trees are by nature immune to multi-collinearity, so we dropped collinear variables in subsequent analyses as this may prevent confusion. Additionally, the relative importance (%) of each explanatory variable derived the optimized BRT model and partial dependency plots (PDP) were adopted to explore the responses between each explanatory variable and g_s, independent of other predictors. All statistical analyses were conducted in R 4.2.1.

2.3.2. Exploring the associations between leaf spectra, stomatal anatomical/behavioral traits, and g_s

After removing collinear variables, we focused on stomatal size and opening ratio for analyzing leaf spectra associations. First, we quantitatively analyzed the associations between leaf spectra and stomatal anatomical/behavioral traits ($n = 361$) using the widely applied partial least squared regression (PLSR) approach. PLSR combines dimensionality reduction techniques similar to principal component analysis and outperforms classical regression approaches due to its capability to handle high predictor collinearity and accommodate a larger number of predictor variables relative to the number of observations (Fonville et al., 2010). Additionally, PLSR accounts for the covariance between the response variable and predictor variables while maintaining the interpretability of linear regression, making it popular for chemometric and spectroscopic analyses (Liu et al., 2023; Serbin et al., 2015; Wu et al., 2019; Yan et al., 2021). In our study, we adopted a repeated double cross-validation (rdCV) PLSR modeling approach (Filzmoser et al., 2009; Yan et al., 2021). The rdCV method first randomly split the full dataset into calibration and independent validation subsets using a cross-validation procedure (outer CV loop) and further divided the calibration subset into training and testing components with a second cross-validation procedure (inner CV loop). The inner CV loop was used to determine the optimal number of latent variables based on performance evaluation, maximizing the averaged R^2 and minimizing the averaged RMSE to avoid model over-fitting. Next, we derived the variable importance in projection (VIP) metric in the inner CV loop and averaged them to obtain the VIP spectrum. PLSR VIP values indicate the relative importance of each wavelength to the PLSR model, retaining the most influential spectral regions when their VIP value exceeded 1 (Wold et al., 2001). The PLSR model was built in the outer CV loop alongside the optimal latent variable number. Model performance was assessed using R^2 for linear regressions between observed and predicted values and RMSE of prediction within independent validation subsets. In total, we performed 100 repetitions for the rdCV and tenfold cross-validation for both the outer and inner CV loops, ultimately contributing an ensemble ($n = 100$) of PLSR models for stomatal size and opening ratio, respectively. Then, we utilized 56 samples obtained from the day-long diurnal sampling campaign to conduct a comparative analysis of the field and spectral-based diurnal variability of g_s. For spectral-based analysis, we also built a PLSR model to investigate the candidate sensitive spectral bands of g_s. This approach enabled us to focus on the sensitive spectra of g_s and also evaluate whether the spectral variations caused by g_s are associated with the spectra alterations induced by stomatal anatomical/behavioral traits.

2.3.3. Exploring the potential links underlying diurnal variations in spectra, behavioral trait and g_s

By comparing the diurnal leaf spectra of the same leaf throughout a single day, we maximally isolated effects of genotype, growth stage, and nitrogen fertilization treatments on leaf spectra. Thus, to explore the potential morphological and biochemical links between stomatal traits and g_s, and leaf spectra across the diurnal dynamics, we analyzed the diurnal variations in leaf reflectance spectra, and the diurnal association of g_s and stomatal behavioral traits with two spectra-derived indices of leaf xanthophyll pigment (PRI_{570}, PRI_{norm}) and two indices related to leaf water content (*LWI* and *MSI*). We used R^2 to assess the associations between each index of xanthophyll pigment and water content, and g_s and behavioral trait.

3. Results

3.1. Associations between stomatal anatomical/behavioral traits and g_s

To address our first question concerning the relationship between stomatal anatomical/behavioral traits and g_s, we examined their individual and combined associations (Fig. 3). Our results show g_s ranged from 0.02 to 37.03 mm s^{-1}, with an average of 11.37 mm s^{-1}. Individual associations based on ordinary least squares regression analysis reveal that stomatal behavioral traits of opening ratio and pore area positively correlate with g_s (Fig. 3c-d, R^2 = 0.57 and 0.49), whereas stomatal anatomical traits of size and density display weak direct relationships (Fig. 3a-b, $R^2 < 0.001$). The BRT model reveals similar patterns, while identifying non-linear correlations for each of these individual associations (Fig. 3e-h). Meanwhile, the BRT model also characterized their joint associations, with all four stomatal metrics collectively having a predictive power of $R^2 = 0.79$ and RMSE = 2.94 mm s^{-1} (Fig. 3i), which is much higher than individual associations, emphasizing the joint influences of the four metrics on g_s. Furthermore, the BRT model demonstrates the relatively significant contributions of stomatal behavioral traits (54.8% for opening ratio and 26.7% for pore area; Fig. 3j) in predicting g_s, compared to stomatal anatomical traits of size and density (total of 18.5%; Fig. 3j). Both opening ratio and pore area show significant relationships with g_s (Fig. 3g-h), while stomatal size and density exhibit near-constant relationships with g_s (Fig. 3e-f). These near-constant relationships, along with the similarity in mean g_s responses to stomatal size (11.66 mm s^{-1}; Fig. 3e) and density (11.42 mm s^{-1}; Fig. 3f) to the mean g_s value (11.37 mm s^{-1}), indicate limited influence of stomatal anatomical traits on g_s variability but constrains on the magnitude of g_s variations. Then, to avoid collinearity and simplify subsequent analysis, we retained stomatal size and opening ratio for anatomical and behavioral traits, as they had a higher relative importance compared to stomatal density and pore area, respectively. A simplified BRT model, only including these two metrics, exhibits similar predictive power ($R^2 = 0.76$, RMSE = 3.16 mm s^{-1}), relative importance (79.1% for opening ratio and 20.9% for stomatal size) and non-linear correlations (Fig. S2), when compared to the scenarios of four metrics (Fig. 3e-j).

3.2. Associations between leaf spectra, stomatal size/opening ratio, and g_s

To address our second question regarding the associations between stomatal size/opening ratio and leaf spectra, we conducted PLSR modeling analyses. Specifically, the leaf spectra-stomatal size PLSR model revealed two sensitive spectral ranges, as indicated by a VIP > 1, and peaked at 553 nm and 707 nm (Fig. 4a). This model demonstrates a strong predictive power, with an R^2 of 0.68 and an RMSE of 0.15 × 10^3 μm^2 (Fig. 4b). Next, we assessed the associations between opening ratio and leaf spectra. The leaf spectra-opening ratio PLSR model infers four core peaks, occurring at 525 nm, 692 nm, 1380 nm, and 1919 nm

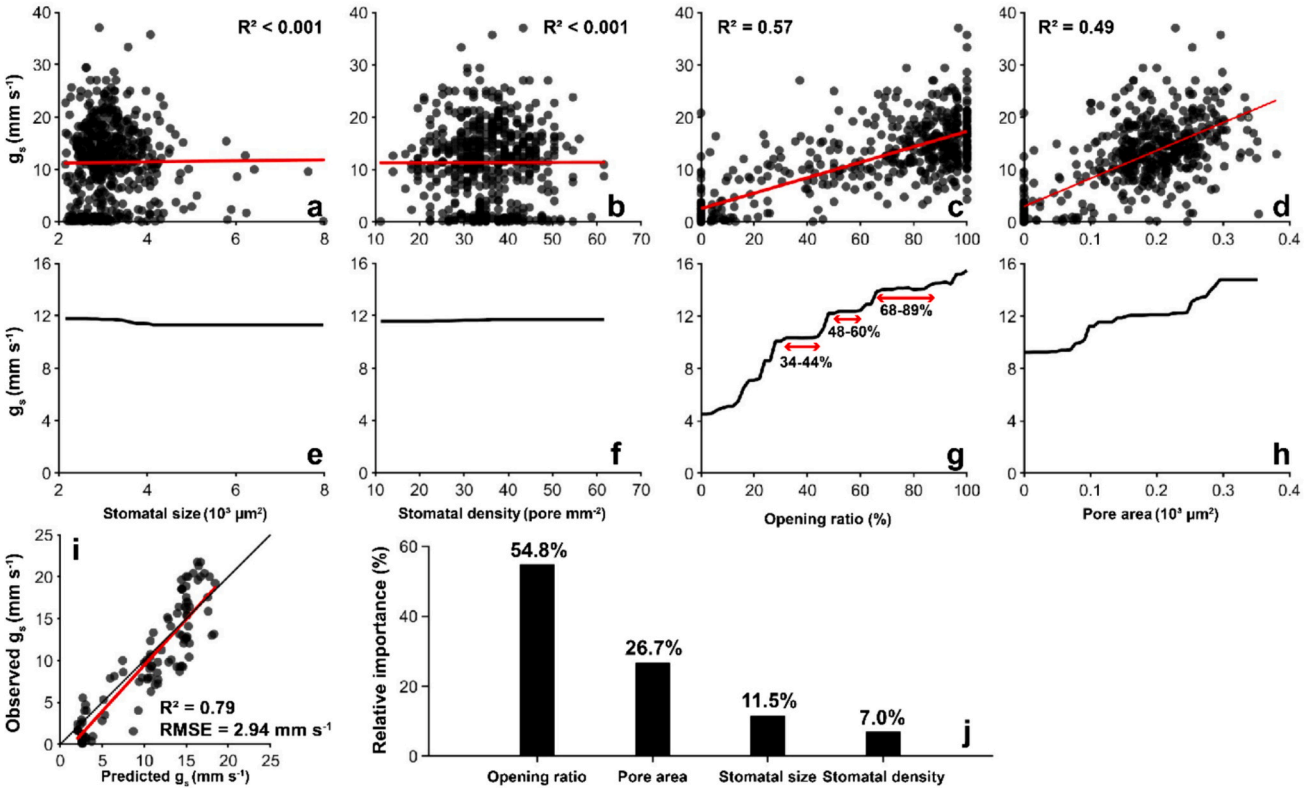

Fig. 3. The relationships between stomatal conductance (g_s) and stomatal anatomical and behavioral traits: (a-d) ordinary least squares regression between g_s and stomatal size, stomatal density, opening ratio and pore area; (e-f) partial dependency plots (PDP) of stomatal size, stomatal density, opening ratio and pore area; (i) g_s BRT model performance; and (j) relative importance (%) of stomatal size, stomatal density, opening ratio and pore area to g_s (j).

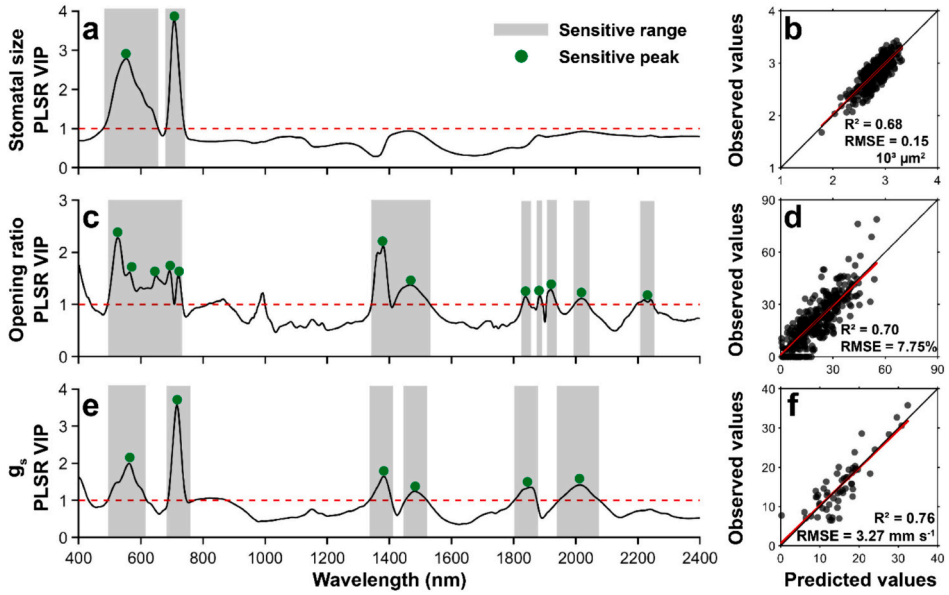

Fig. 4. Variable importance in projection of partial least-squares regression (PLSR VIP) and PLSR model performance: (a) PLSR VIP of stomatal size; (b) model performance of stomatal size; (c) PLSR VIP of opening ratio; (d) model performance of opening ratio; (e) PLSR VIP of stomatal conductance (g_s); and (f) model performance of g_s.

(Fig. 4c). In addition to these peaks, the PLSR model also identified several other minor spectral sensitive domains, featuring peaks at various wavelengths of 650 nm, 721 nm, 865 nm, 993 nm, 1466 nm, 1838 nm, 1884 nm, 2018 nm, and 2220 nm. The leaf spectra-opening ratio PLSR model demonstrates a robust predictive performance, with an R^2 of 0.70 and RMSE of 7.75% (Fig. 4d). Thus, our study effectively demonstrates strong associations between leaf spectra and stomatal size/opening ratio and shows that leaf spectra alone can accurately infer both stomatal size and opening ratio through the application of the PLSR model. Next, we analyzed the seven-revisit spectral variances of the same single leaf for each genotype × nitrogen treatment combination across the full diurnal condition. Comparing the same single leaf enables a rigorous analysis of spectral effects induced by diurnal dynamics, as we have isolated effects of genotype, growth stage and nitrogen fertilization treatments on the spectra. Using the diurnal g_s data, the leaf spectra-g_s PLSR model also demonstrates a strong predictive power, with an R^2 of 0.76 and an RMSE of 3.27 mm s^{-1} (Fig. 4f), significantly illustrating that spectra can mirror diurnal variations of g_s. Six peaks are identified by a VIP > 1, including 562 nm, 716 nm, 1382 nm, 1482 nm, 1854 nm, and 2013 nm (Fig. 4e). Notably, these six sensitive spectral ranges (including peaks) of g_s, indicated by the VIP of the leaf spectra-g_s PLSR model, are encompassed by the sensitive spectral regions of stomatal size and opening ratio that have been identified by the leaf spectra-size and leaf spectra-opening ratio PLSR models. Specifically, within the visible-NIR bands (400–1000 nm), two sensitive spectral ranges of g_s almost coincide with those of stomatal size, and the peaks are also recognized by those of stomatal opening ratio. The remaining four sensitive spectral ranges of g_s within the NIR-SWIR range are captured by those of opening ratio. Overall, these results show that wavelength-specific variation in reflectance is associated with changes induced by stomatal size and opening ratio, and when combined, the same spectral regions are similarly associated with g_s. This suggests that spectral monitoring of g_s appears to be directly mediated by both stomatal anatomical and behavioral traits.

3.3. The potential morphological and biochemical links between opening ratio, g_s, and leaf spectra

We observed that the sensitive spectral ranges identified for opening ratio and g_s in our PLSR models bear resemblance to the sensitive spectral domains for leaf xanthophyll pigment and leaf water content. This suggests that the impact of opening ratio and g_s variations on spectra is akin to the effects of leaf xanthophyll pigment and water content on spectra. To quantify their relationships, we analyzed the correlations between opening ratio, g_s, and the indices of xanthophyll pigment (PRI_{570}, PRI_{norm}) and leaf water content (*LWI*, *MSI*) for each genotype × nitrogen fertilization treatment combination (Fig. 5). Overall, leaf g_s demonstrates a stronger correlation with these indices than the correlation between opening ratio and indices. Specifically, the correlation between g_s and PRI_{570}/PRI_{norm} for most combinations is relatively good, except GT5(N240), with R^2 values ranging from 0.18 to 0.90 (Fig. 5a). In contrast, the correlation between opening ratio and PRI_{570}/PRI_{norm} is somewhat weaker, with R^2 values ranging from 0.14 to 0.69 (Fig. 5b) when excluding GT2(N240) and GT3(N0). Regarding leaf water content indices, LWI exhibits a better performance for both g_s and opening ratio. The R^2 for the correlation between g_s and *LWI* ranges from 0.27 to 0.67 (Fig. 5a), while the R^2 range for the correlation between opening ratio and *LWI* is 0.08–0.73 (Fig. 5b). Subsequently, we calculated the mean of PRI_{norm}, *LWI*, g_s and opening ratio from eight combinations to further elucidate the relationships between leaf spectra and g_s as well as opening ratio, with the goal of evaluating the feasibility of leaf spectra for monitoring diurnal dynamics of g_s and opening ratio (Fig. 6). Generally, leaf g_s is highest in the morning and decreases in the afternoon, followed by a minor increase occurring in the last sampling round at around 6 pm local time (Fig. 6a&c). The opening ratio exhibits similar diurnal patterns with g_s (Fig. 6b&d), further emphasizing the role of stomatal behavioral trait in regulating g_s on a diurnal scale.

4. Discussion

In this study, we present three key findings. First, our results reveal significant variability in *in-vivo* g_s, with 79% of this variability attributed to the combined influence of stomatal anatomical and behavioral traits. Second, we demonstrate that single leaf hyperspectral reflectance measurements enable accurate tracking of stomatal anatomical/behavioral traits and g_s, and the sensitive spectral variations identified by the spectral model for g_s exhibit a strong correspondence with the reflectance changes induced by stomatal anatomical and behavioral traits. Third, our study uncovers significant variations in leaf reflectance spectra for the same leaves across a diurnal scale, and such diurnal

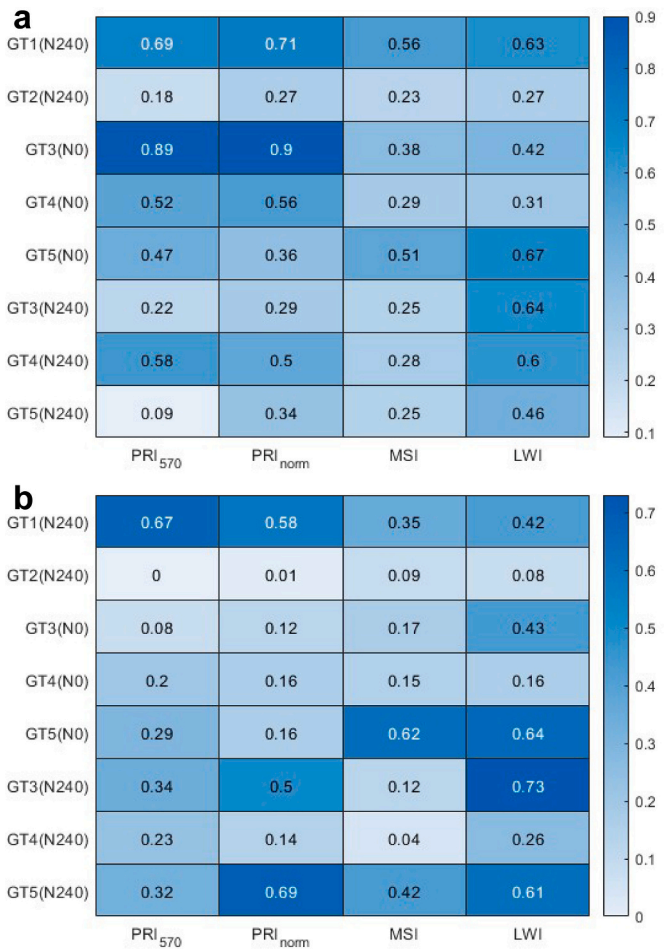

Fig. 5. The coefficients of determination (R^2) between stomatal conductance (g_s) and opening ratio, and the indices of xanthophyll pigment (PRI_{570} and PRI_{norm}) and leaf water content (*LWI* and *MSI*) for each combination of genotype × nitrogen fertilization treatment: (a) g_s and (b) opening ratio. GT denotes genotype, N240 denotes the nitrogen fertilization treatment is 240 kg/ha and N0 denotes the nitrogen fertilization treatment is 0 kg/ha.

dynamics of leaf spectra can effectively monitor g_s and stomatal opening ratio at a diurnal scale, displaying strong underlying biochemical associations between spectra-derived leaf water content and xanthophyll pigment with g_s and stomatal opening ratio. Collectively, our study provides a comprehensive assessment on the relationships between leaf spectra, stomatal anatomical/behavioral traits, and g_s, highlighting the fundamental biological mechanisms underlying spectral sensing of g_s.

We observe that stomatal behavioral traits, rather than anatomical traits, predominantly regulate *in-vivo* g_s dynamics. This finding is based on field datasets collected from diverse wheat genotypes, growth stages, and diurnal environmental conditions, with leaf g_s data covering a wide value range of ~0–40 mm s^{-1}, comparable to previous studies (Jiao et al., 2018; Xu et al., 2018; Yan et al., 2023). This observation aligns with prior research, which suggested that stomatal anatomical traits typically determine a plant's theoretical maximum g_s rather than its actual/measured g_s (Faralli et al., 2019). Consequently, it is expected that stomatal anatomical traits alone have limited explanatory power for g_s dynamics, while other processes beyond stomatal anatomical traits, such as stomatal behavioral traits triggered by ambient environmental conditions (Dow et al., 2014), more importantly regulate *in-vivo* g_s dynamics. Our study provides, to the best of our knowledge, the first direct quantitative assessment of the roles of stomatal anatomical and behavioral traits in regulating g_s dynamics. This novel finding is made possible because we integrate a cutting-edge microscopy imaging system with deep learning (Sun et al., 2023), enabling accurate, *in-vivo* monitoring of stomatal behavioral traits, data that have been rarely available previously.

Given that both stomatal anatomical and behavioral traits contribute to *in-vivo* g_s dynamics, we further investigate whether leaf spectra exhibit significant and distinct associations with these traits. By controlling the impacts of stomatal anatomical and behavioral traits separately, our results clearly demonstrate their unique spectral associations. For example, stomatal size displays significant spectral associations across multiple regions in the visible light domain (*i.e.*, 553 nm, 707 nm). Notably, these sensitive spectral regions strongly coincide with sensitive spectral regions for leaf chlorophyll pigment (550–560 nm, 680–740 nm) (Datt, 1998; Gitelson and Merzlyak, 1996). One possible reason for this coincidence could be the co-evolution of plant physiological processes of photosynthetic capacity (related with maximum light absorption by leaf chlorophyll content) and transpiration capacity (related with maximum g_s mediated by stomatal size) (Reich et al., 2003; Wright et al., 2004). However, future research remains needed for a more in-depth exploration of the coordinated relationship between them.

Similarly, we identify several sensitive spectral regions related to the opening ratio, which include three peaks (525 nm, 650 nm and 692 nm) in the visible range, as well as additional peaks (721 nm, 865 nm, 993 nm, 1380 nm, 1466 nm, 1838 nm, 1884 nm, 1919 nm, 2018 nm and 2220 nm) in the near-infrared and shortwave-infrared ranges (Fig. 4). To our knowledge, these sensitive spectral regions have not been previously reported, primarily due to the lack of paired datasets encompassing both leaf spectra and stomatal behavioral traits. Furthermore, we find that these identified sensitive spectral bands bare similarities to sensitive

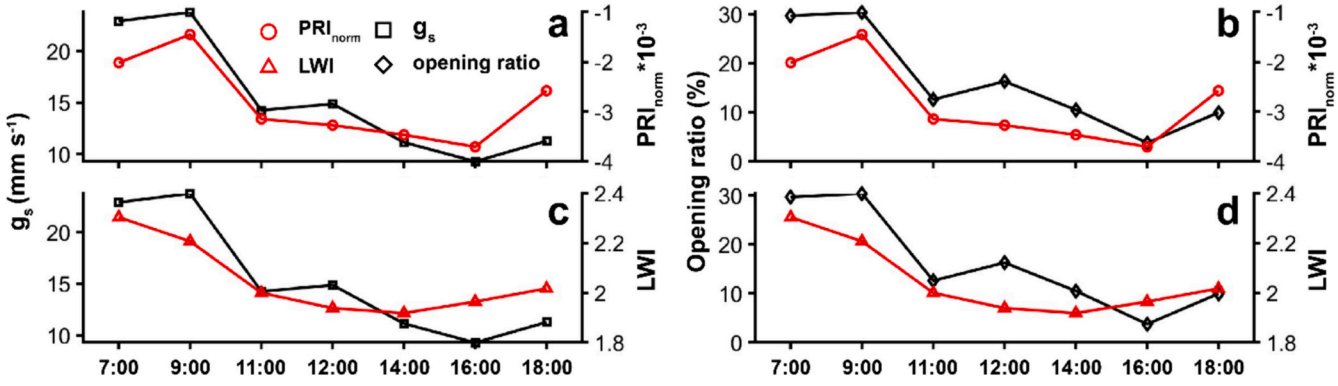

Fig. 6. Diurnal dynamics of stomatal conductance (g_s), opening ratio, normalized photochemical reflectance index (PRI_{norm}) and leaf water index (*LWI*): (a) g_s and PRI_{norm}; (b) opening ratio and PRI_{norm}; (c) g_s and *LWI*; and (d) opening ratio and *LWI*. Data are the averaged values from eight combinations of genotype × nitrogen fertilization treatment.

spectral domains associated with xanthophyll pigments (400–531 nm) and leaf water content (near 1450 nm, and 1950–1980 nm) (Curran, 1989; Datt, 1999; El-Hendawy et al., 2019; Sims and Gamon, 2002). Following this observation, we next quantitatively assess the diurnal variations in spectra-derived indices of xanthophyll pigments and leaf water content, discovering positive correlations between these two indices and the opening ratio (Figs. 5b, 6b&d). This finding suggests that the ability of leaf spectra to monitor g_s and stomatal behavioral traits may arise from their direct associations with leaf spectra, but even more likely due to diurnal or environmentally induced changes in internal leaf properties (such as xanthophyll pigments and leaf water content) related to stomatal activities that exhibit direct sensitivity to leaf spectral changes. Apart from xanthophyll pigments and leaf water content-induced spectral changes throughout diurnal condition, our spectra-based PLSR model also identifies several sensitive spectral regions around 2000–2200 nm, where certain metabolites and proteins also demonstrate sensitivity (Bright et al., 2006; Burnett et al., 2021). For example, drought-induced proteins and metabolites linked to the leaf water stress such as abscisic acid and proline, exhibit significant spectral features in near 1980 nm and within the 1400–2500 nm range (Bright et al., 2006; Burnett et al., 2021). However, further biochemical or molecular evidence is required to elucidate such stress-induced spectral association with stomatal opening ratio in future research.

While leaf/canopy reflectance spectra have demonstrated their capability to characterize leaf biochemical, morphological, and physiological traits at seasonal or inter-annual scales due to recent advancement in vegetation spectroscopy studies (Chen et al., 2022; Sobejano-Paz et al., 2020; Wu et al., 2019; Yang et al., 2014, 2016), the direct application of leaf spectra for sensing plant physiology at a diurnal scale remain contentious. This uncertainty is attributed to plant physiological rates (*i.e.*, photosynthesis, respiration, and transpiration), which can exhibit instantaneous responses to ambient environmental changes, resulting in significant diurnal variations (Guo et al., 2022, 2023). However, leaf biochemical (*i.e.*, chlorophyll content) and physiological (*i.e.*, photosynthetic capacity) traits, which are crucial biotic controls of plant physiological rates, barely change within a day. Additionally, previous seasonal or even longer-time scale studies on the relationship between spectra, leaf traits and physiological rates provide limited insight into their diurnal associations (Wu et al., 2016, 2017; Xia et al., 2015). Our novel discovery of diurnal variations in leaf spectra and their close associations with g_s and stomatal behavioral traits (opening ratio) provides direct evidence that leaf spectra can effectively monitor diurnal plant physiological activities, addressing this knowledge gap. Moreover, our results are consistent with Serbin et al. (2012) that observed significant leaf spectral changes in response to ambient temperature change, suggesting that leaf spectra could serve as an effective alternative for directly sensing plant photosynthesis rates (approximated by photosynthetic capacity, V_{cmax}). Collectively, these findings indicate that leaf spectra indeed hold the potential to advance the monitoring of plant physiological activities such as photosynthesis (Serbin et al., 2012) and stomatal regulation (this study), and potentially many others.

In addition to the potential mechanisms underlying the associations among spectra, stomatal anatomical/behavioral traits, and g_s as discussed above, our results also demonstrate that single spectral models offer a rapid, accurate, scalable, and non-destructive alternative for monitoring stomatal size ($R^2 = 0.68$; Fig. 4b), stomatal opening ration ($R^2 = 0.70$; Fig. 4d), and g_s ($R^2 = 0.76$; Fig. 4f). This finding is significant, as it suggests that leaf spectra can not only infer g_s but also key stomatal traits underlying g_s regulation. This provides valuable paired datasets to interpret the interplay among ambient environments, stomatal anatomical/behavioral traits, and g_s, essential for understanding crop sensitivity to climate change. Notably, monitoring stomatal behavioral traits *in-vivo* have been notoriously challenging. The high predictive accuracy of stomatal opening ratio revealed in our study highlights the potential of leaf spectra for effectively characterizing stomatal opening behavior, complementing the microscopy imaging approach as used in this study (Sun et al., 2023). Several recent studies (El-Hendawy et al., 2019; Shahrimie et al., 2022; Sobejano-Paz et al., 2020) also demonstrated the high accuracy of using leaf/plant spectra to characterize gs, aligning with our findings. However, our study differs by showcasing the high-throughput capability of using leaf spectra for characterizing both g_s and associated underlying stomatal traits, and offering candidate mechanisms underlying the associations among leaf spectra, stomatal traits, and g_s. These results collectively provide a significant biological foundation for the spectral sensing of g_s.

Our findings have two broader implications for vegetation spectroscopy and crop physiology studies. Firstly, our research complements existing spectral physiology studies by showcasing the potential of leaf spectroscopy for characterizing stomatal anatomical and behavioral traits. These traits are typically challenging to study *in-vivo* due to scale constraints of imaging spectroscopy or the limitations of destructive measurements. In contrast, leaf spectroscopy provides a high-throughput means for analyzing various leaf traits and their relationships (Sobejano-Paz et al., 2020; Wu et al., 2019; Yan et al., 2021; Yang et al., 2016). In conjunction with our findings, spectroscopy enables high-throughput characterization of even more traits, collectively providing a comprehensive understanding of the interplay among multiple trait dimensions. Secondly, our findings hold potential for providing valuable complementary datasets that enhance our understanding of crop sensitivity response (particularly through stomatal regulation) to nutrient deficiency and other environmental stressors. These insights are crucial for addressing current-day food security problems, as these stressors pose significant risks to crop yield, ultimately affecting agricultural productivity and sustainability. Characterizing stomatal regulation traits through spectroscopy can be an effective way to obtain high-resolution data that may help identify key factors for stress resistance and resilience. Such data could prove invaluable in assisting in crop breeding programs or developing accurate crop models for informed agricultural management and policy decisions.

Our study has limitations, such as focusing on a single crop and leaf-level measurements, lacking insights from various crops at canopy/ecosystem scales. Exploring these aspects could provide new insights for revealing plant growth, adaptation, and resilience to stressors, ultimately promoting sustainable agricultural productivity and ecosystem health (Lobell et al., 2003). To address these limitations, future research should encompass a wider range of crops and ecosystems, enabling more comprehensive models and techniques for larger scales, benefiting diverse agricultural and environmental management practices. The potential extension to various crops and scaling-up to larger canopy and ecosystem levels is highly plausible, as similar approaches have already been employed in managed agricultural sites (Serbin et al., 2015). Advanced imaging spectroscopy techniques, such as the imaging system onboard unmanned aerial vehicles, offer the potential for high-resolution, non-destructive measurements of plant properties, physiological processes, and responses to environmental stressors at the canopy level. This would allow for a more accurate representation of plant functioning at larger scales, ultimately enhancing our understanding of plant functioning and stress responses in diverse agricultural and natural ecosystems.

CRediT authorship contribution statement

K.H. Cheng: Data curation, Formal analysis, Investigation, Methodology, Validation, Writing – original draft, Conceptualization, Visualization. **Zhuangzhuang Sun:** Formal analysis, Investigation, Methodology, Software, Writing – review & editing. **Wanlu Zhong:** Investigation, Writing – review & editing. **Zhihui Wang:** Data curation, Funding acquisition, Investigation, Writing – review & editing. **Marco Visser:** Funding acquisition, Writing – review & editing. **Shuwen Liu:** Methodology, Writing – review & editing. **Zhengbing Yan:** Investigation, Methodology, Writing – review & editing. **Yingyi Zhao:**

Methodology, Writing – review & editing. **Ruinan Zhang:** Investigation, Writing – review & editing. **Jingrong Zang:** Methodology, Writing – review & editing. **Shichao Jin:** Funding acquisition, Investigation, Writing – review & editing. **Jin Wu:** Conceptualization, Funding acquisition, Supervision, Writing – review & editing, Data curation, Investigation, Methodology, Project administration, Resources, Visualization.

Declaration of competing interest

The authors declare that they have no known competing financial interests or personal relationships that could have appeared to influence the work reported in this paper.

Data availability

The data that support the findings of this study are openly available in figshare at https://doi.org/10.6084/m9.figshare.24137937.v1.

Acknowledgements

This work was supported by National Natural Science Foundation of China (#31922090), the HKU Seed Funding for Strategic Interdisciplinary Research Scheme, Hong Kong Research Grant Council Collaborative Research Fund (#C5062-21GF), the Innovation and Technology Fund (funding support to State Key Laboratories in Hong Kong of Agrobiotechnology) of the HKSAR, China, GDAS' Special Project of Science and Technology Development (2020GDASYL-20200102001), Jiangsu Agricultural Science and Technology Independent Innovation Fund Project (No. CX(21)3107), High Level Personnel Project of Jiangsu Province (JSSCBS20210271), the CML impact fund at Leiden University.

Appendix A. Supplementary data

Supplementary data to this article can be found online at https://doi.org/10.1016/j.rse.2024.114325.

References

Bright, J., Desikan, R., Hancock, J.T., Weir, I.S., Neill, S.J., 2006. ABA-induced NO generation and stomatal closure in Arabidopsis are dependent on H2O2 synthesis. Plant J. 45, 113–122. https://doi.org/10.1111/j.1365-313X.2005.02615.x.

Brodribb, T.J., McAdam, S.A.M., 2017. Evolution of the stomatal regulation of plant water content. Plant Physiol. 174, 639–649. https://doi.org/10.1104/pp.17.00078.

Buckley, T.N., 2017. Modeling stomatal conductance. Plant Physiol. 174, 572–582. https://doi.org/10.1104/pp.16.01772.

Buckley, T.N., Sack, L., Gilbert, M.E., 2011. The role of bundle sheath extensions and life form in stomatal responses to leaf water status. Plant Physiol. 156, 962–973. https://doi.org/10.1104/pp.111.175638.

Burnett, A.C., Serbin, S.P., Davidson, K.J., Ely, K.S., Rogers, A., 2021. Detection of the metabolic response to drought stress using hyperspectral reflectance. J. Exp. Bot. 72, 6474–6489.

Chen, L., Zhang, Y., Nunes, M.H., Stoddart, J., Khoury, S., Chan, A.H.Y., Coomes, D.A., 2022. Predicting leaf traits of temperate broadleaf deciduous trees from hyperspectral reflectance: can a general model be applied across a growing season? Remote Sens. Environ. 269, 112767.

Coast, O., Shah, S., Ivakov, A., Gaju, O., Wilson, P.B., Posch, B.C., Bryant, C.J., Negrini, A.C.A., Evans, J.R., Condon, A.G., 2019. Predicting dark respiration rates of wheat leaves from hyperspectral reflectance. Plant Cell Environ. 42, 2133–2150.

Curran, P.J., 1989. Remote sensing of foliar chemistry. Remote Sens. Environ. 30, 271–278.

Datt, B., 1998. Remote sensing of chlorophyll a, chlorophyll b, chlorophyll a+ b, and total carotenoid content in eucalyptus leaves. Remote Sens. Environ. 66, 111–121.

Datt, B., 1999. Remote sensing of water content in Eucalyptus leaves. Aust. J. Bot. 47, 909–923.

Dayer, S., Herrera, J.C., Dai, Z., Burlett, R., Lamarque, L.J., Delzon, S., Bortolami, G., Cochard, H., Gambetta, G.A., 2020. The sequence and thresholds of leaf hydraulic traits underlying grapevine varietal differences in drought tolerance. J. Exp. Bot. 71, 4333–4344.

Dhankher, O.P., Foyer, C.H., 2018. Climate resilient crops for improving global food security and safety. Plant, Cell & Environment 41 (5), 877–884.

Ding, H., Wang, Z., Zhang, Y., Li, J., Jia, L., Chen, Q., Ding, Y., Wang, S., 2023. A mechanistic model for estimating Rice photosynthetic capacity and stomatal conductance from Sun-induced chlorophyll fluorescence. Plant Phenom. 5, 47.

Dow, G.J., Bergmann, D.C., Berry, J.A., 2014. An integrated model of stomatal development and leaf physiology. New Phytol. 201, 1218–1226.

El-Hendawy, S.E., Al-Suhaibani, N.A., Hassan, W.M., Dewir, Y.H., Elsayed, S., Al-Ashkar, I., Abdella, K.A., Schmidhalter, U., 2019. Evaluation of wavelengths and spectral reflectance indices for high-throughput assessment of growth, water relations and ion contents of wheat irrigated with saline water. Agric. Water Manag. 212, 358–377.

Elith, J., Leathwick, J.R., Hastie, T., 2008. A working guide to boosted regression trees. J. Anim. Ecol. 77, 802–813.

Faralli, M., Matthews, J., Lawson, T., 2019. Exploiting natural variation and genetic manipulation of stomatal conductance for crop improvement. Curr. Opin. Plant Biol. 49, 1–7.

Faralli, M., Bontempo, L., Bianchedi, P.L., Moser, C., Bertamini, M., Lawson, T., Camin, F., Stefanini, M., Varotto, C., 2022. Natural variation in stomatal dynamics drives divergence in heat stress tolerance and contributes to seasonal intrinsic water-use efficiency in Vitis vinifera (subsp. sativa and sylvestris). J. Exp. Bot. 73, 3238–3250.

Filzmoser, P., Liebmann, B., Varmuza, K., 2009. Repeated double cross validation. J. Chemom. A J. Chemom. Soc. 23, 160–171.

Fonville, J.M., Richards, S.E., Barton, R.H., Boulange, C.L., Ebbels, T.M.D., Nicholson, J. K., Holmes, E., Dumas, M., 2010. The evolution of partial least squares models and related chemometric approaches in metabonomics and metabolic phenotyping. J. Chemom. 24, 636–649.

Franks, P.J., Beerling, D.J., 2009. Maximum leaf conductance driven by CO2 effects on stomatal size and density over geologic time. Proc. Natl. Acad. Sci. 106, 10343–10347.

Fu, P., Meacham-Hensold, K., Guan, K., Wu, J., Bernacchi, C., 2020. Estimating photosynthetic traits from reflectance spectra: a synthesis of spectral indices, numerical inversion, and partial least square regression. Plant Cell Environ. 43, 1241–1258.

Galmés, J., Ochogavía, J.M., Gago, J., Roldán, E.J., Cifre, J., Conesa, M.À., 2013. Leaf responses to drought stress in Mediterranean accessions of Solanum lycopersicum: anatomical adaptations in relation to gas exchange parameters. Plant Cell Environ. 36, 920–935.

Gamon, J.A., Surfus, J.S., 1999. Assessing leaf pigment content and activity with a reflectometer. New Phytol. 143, 105–117.

Gamon, J.A., Penuelas, J., Field, C.B., 1992. A narrow-waveband spectral index that tracks diurnal changes in photosynthetic efficiency. Remote Sens. Environ. 41, 35–44.

Gitelson, A.A., Merzlyak, M.N., 1996. Signature analysis of leaf reflectance spectra: algorithm development for remote sensing of chlorophyll. J. Plant Physiol. 148, 494–500.

Gong, X., Ma, L., Ouyang, H., 2020. An improved method of tiny YOLOV3. In: IOP Conference Series: Earth and Environmental Science. IOP Publishing, p. 52025.

Greenwell, B., Boehmke, B., Cunningham, J., Developers, G.B.M., Greenwell, M.B., 2019. Package 'gbm'. R Packag. version 2.

Guo, Z., Yan, Z., Majcher, B.M., Lee, C.K.F., Zhao, Y., Song, G., Wang, B., Wang, X., Deng, Y., Michaletz, S.T., 2022. Dynamic biotic controls of leaf thermoregulation across the diel timescale. Agric. For. Meteorol. 315, 108827.

Guo, Z., Zhang, K., Lin, H., Majcher, B.M., Lee, C.K.F., Still, C.J., Wu, J., 2023. Plant canopies exhibit stronger thermoregulation capability at the seasonal than diurnal timescales. Agric. For. Meteorol. 339, 109582.

Haile, M., 2005. Weather patterns, food security and humanitarian response in sub-Saharan Africa. Philos. Trans. R. Soc. B Biol. Sci. 360, 2169–2182.

Hetherington, A.M., Woodward, F.I., 2003. The role of stomata in sensing and driving environmental change. Nature 424, 901–908.

Hunt Jr., E.R., Rock, B.N., 1989. Detection of changes in leaf water content using near- and middle-infrared reflectances. Remote Sens. Environ. 30, 43–54.

Jiao, L., Ding, R., Kang, S., Du, T., Tong, L., Li, S., 2018. A comparison of energy partitioning and evapotranspiration over closed maize and sparse grapevine canopies in Northwest China. Agric. Water Manag. 203, 251–260.

Jin, J., Yan, T., Wang, H., Ma, X., He, M., Wang, Y., Wang, W., Guo, F., Cai, Y., Zhu, Q., 2022. Improved modeling of canopy transpiration for temperate forests by incorporating a LAI-based dynamic parametrization scheme of stomatal slope. Agric. For. Meteorol. 326, 109157.

Kokaly, R.F., Asner, G.P., Ollinger, S.V., Martin, M.E., Wessman, C.A., 2009. Characterizing canopy biochemistry from imaging spectroscopy and its application to ecosystem studies. Remote Sens. Environ. 113, S78–S91.

Liang, X., Xu, X., Wang, Z., He, L., Zhang, K., Liang, B., Ye, J., Shi, J., Wu, X., Dai, M., 2022. StomataScorer: a portable and high-throughput leaf stomata trait scorer combined with deep learning and an improved CV model. Plant Biotechnol. J. 20, 577–591.

Lin, Y.-S., Medlyn, B.E., Duursma, R.A., Prentice, I.C., Wang, H., Baig, S., Eamus, D., De Dios, V.R., Mitchell, P., Ellsworth, D.S., 2015. Optimal stomatal behaviour around the world. Nat. Clim. Chang. 5, 459–464.

Liu, S., Yan, Z., Wang, Z., Serbin, S., Visser, M., Zeng, Y., Ryu, Y., Su, Y., Guo, Z., Song, G., 2023. Mapping foliar photosynthetic capacity in sub-tropical and tropical forests with UAS-based imaging spectroscopy: scaling from leaf to canopy. Remote Sens. Environ. 293, 113612.

Lobell, D.B., Asner, G.P., Ortiz-Monasterio, J.I., Benning, T.L., 2003. Remote sensing of regional crop production in the Yaqui Valley, Mexico: estimates and uncertainties. Agric. Ecosyst. Environ. 94, 205–220.

Mantzoukas, S., Chondrogiannis, C., Grammatikopoulos, G., 2015. Effects of three endophytic entomopathogens on sweet sorghum and on the larvae of the stalk borer S esamia nonagrioides. Entomol. Exp. Appl. 154, 78–87.

McAusland, L., Vialet-Chabrand, S., Davey, P., Baker, N.R., Brendel, O., Lawson, T., 2016. Effects of kinetics of light-induced stomatal responses on photosynthesis and water-use efficiency. New Phytol. 211, 1209–1220.
Meacham-Hensold, K., Fu, P., Wu, J., Serbin, S., Montes, C.M., Ainsworth, E., Guan, K., Dracup, E., Pederson, T., Driever, S., 2020. Plot-level rapid screening for photosynthetic parameters using proximal hyperspectral imaging. J. Exp. Bot. 71, 2312–2328.
Medlyn, B.E., Duursma, R.A., Eamus, D., Ellsworth, D.S., Prentice, I.C., Barton, C.V.M., Crous, K.Y., De Angelis, P., Freeman, M., Wingate, L., 2011. Reconciling the optimal and empirical approaches to modelling stomatal conductance. Glob. Chang. Biol. 17, 2134–2144.
Medlyn, B.E., De Kauwe, M.G., Lin, Y., Knauer, J., Duursma, R.A., Williams, C.A., Arneth, A., Clement, R., Isaac, P., Limousin, J., 2017. How do leaf and ecosystem measures of water-use efficiency compare? New Phytol. 216, 758–770.
Mott, K.A., Buckley, T.N., 1998. Stomatal heterogeneity. J. Exp. Bot. 49, 407–417. https://doi.org/10.1093/jxb/49.special_issue.407.
O'Leary, B.M., Scafaro, A.P., York, L.M., 2023. High-throughput, dynamic, multi-dimensional: an expanding repertoire of plant respiration measurements. Plant Physiol. 191, 2070–2083.
Ollinger, S.V., 2011. Sources of variability in canopy reflectance and the convergent properties of plants. New Phytol. 189, 375–394.
Perez-Priego, O., Katul, G., Reichstein, M., El-Madany, T.S., Ahrens, B., Carrara, A., Scanlon, T.M., Migliavacca, M., 2018. Partitioning Eddy covariance water flux components using physiological and micrometeorological approaches. J. Geophys. Res. Biogeosci. 123, 3353–3370. https://doi.org/10.1029/2018JG004637.
Reich, P.B., Wright, I.J., Cavender-Bares, J., Craine, J.M., Oleksyn, J., Westoby, M., Walters, M.B., 2003. The evolution of plant functional variation: traits, spectra, and strategies. Int. J. Plant Sci. 164, S143–S164.
Schweiger, A.K., Cavender-Bares, J., Townsend, P.A., Hobbie, S.E., Madritch, M.D., Wang, R., Tilman, D., Gamon, J.A., 2018. Plant spectral diversity integrates functional and phylogenetic components of biodiversity and predicts ecosystem function. Nat. Ecol. Evol. 2, 976–982.
Seelig, H.-D., Hoehn, A., Stodieck, L.S., Klaus, D.M., Adams, W.W., Emery, W.J., 2009. Plant water parameters and the remote sensing R 1300/R 1450 leaf water index: controlled condition dynamics during the development of water deficit stress. Irrig. Sci. 27, 357–365.
Serbin, S.P., Dillaway, D.N., Kruger, E.L., Townsend, P.A., 2012. Leaf optical properties reflect variation in photosynthetic metabolism and its sensitivity to temperature. J. Exp. Bot. 63, 489–502.
Serbin, S.P., Singh, A., Desai, A.R., Dubois, S.G., Jablonski, A.D., Kingdon, C.C., Kruger, E.L., Townsend, P.A., 2015. Remotely estimating photosynthetic capacity, and its response to temperature, in vegetation canopies using imaging spectroscopy. Remote Sens. Environ. 167, 78–87.
Serbin, S.P., Wu, J., Ely, K.S., Kruger, E.L., Townsend, P.A., Meng, R., Wolfe, B.T., Chlus, A., Wang, Z., Rogers, A., 2019. From the Arctic to the tropics: multibiome prediction of leaf mass per area using leaf reflectance. New Phytol. 224, 1557–1568.
Shabala, S., Hariadi, Y., Jacobsen, S.-E., 2013. Genotypic difference in salinity tolerance in quinoa is determined by differential control of xylem Na+ loading and stomatal density. J. Plant Physiol. 170, 906–914.
Shahrimie, M., Asaari, M., Mertens, S., Verbraeken, L., Dhondt, S., Inzé, D., Bikram, K., Scheunders, P., 2022. Non-destructive analysis of plant physiological traits using hyperspectral imaging: a case study on drought stress, 195. Elsevier, 106806. https://doi.org/10.1016/j.compag.2022.106806.
Sims, D.A., Gamon, J.A., 2002. Relationships between leaf pigment content and spectral reflectance across a wide range of species, leaf structures and developmental stages. Remote Sens. Environ. 81, 337–354.
Sobejano-Paz, V., Mikkelsen, T.N., Baum, A., Mo, X., Liu, S., Köppl, C.J., Johnson, M.S., Gulyas, L., García, M., 2020. Hyperspectral and thermal sensing of stomatal conductance, transpiration, and photosynthesis for soybean and maize under drought. Remote Sens. 12, 3182.
Sporbert, M., Jakubka, D., Bucher, S.F., Hensen, I., Freiberg, M., Heubach, K., König, A., Nordt, B., Plos, C., Blinova, I., 2022. Functional traits influence patterns in vegetative and reproductive plant phenology–a multi-botanical garden study. New Phytol. 235, 2199–2210.
Sun, Z., Wang, X., Song, Y., Li, Q., Song, J., Cai, J., Zhou, Q., Zhong, Y., Jin, S., Jiang, D., 2023. StomataTracker: revealing circadian rhythms of wheat stomata with in-situ video and deep learning. Comput. Electron. Agric. 212, 108120.
Vitrack-Tamam, S., Holtzman, L., Dagan, R., Levi, S., Tadmor, Y., Azizi, T., Rabinovitz, O., Naor, A., Liran, O., 2020. Random forest algorithm improves detection of physiological activity embedded within reflectance spectra using stomatal conductance as a test case. Remote Sens. 12, 2213.
Wang, Z., Wang, C., Wang, X., Wang, B., Wu, J., Liu, L., 2022. Aerosol pollution alters the diurnal dynamics of sun and shade leaf photosynthesis through different mechanisms. Plant Cell Environ. 45, 2943–2953.
Wheeler, T., Von Braun, J., 2013. Climate change impacts on global food security. Science 341, 508–513.
Wold, S., Sjöström, M., Eriksson, L., 2001. PLS-regression: a basic tool of chemometrics. Chemom. Intell. Lab. Syst. 58, 109–130.
Wong, S.C., Cowan, I.R., Farquhar, G.D., 1979. Stomatal conductance correlates with photosynthetic capacity. Nature 282, 424–426.
Wright, I.J., Reich, P.B., Westoby, M., Ackerly, D.D., Baruch, Z., Bongers, F., Cavender-Bares, J., Chapin, T., Cornelissen, J.H.C., Diemer, M., 2004. The worldwide leaf economics spectrum. Nature 428, 821–827.
Wu, J., Albert, L.P., Lopes, A.P., Restrepo-Coupe, N., Hayek, M., Wiedemann, K.T., Guan, K., Stark, S.C., Christoffersen, B., Prohaska, N., 2016. Leaf development and demography explain photosynthetic seasonality in Amazon evergreen forests. Science 351, 972–976.
Wu, J., Guan, K., Hayek, M., Restrepo-Coupe, N., Wiedemann, K.T., Xu, X., Wehr, R., Christoffersen, B.O., Miao, G., Da Silva, R., 2017. Partitioning controls on Amazon forest photosynthesis between environmental and biotic factors at hourly to interannual timescales. Glob. Chang. Biol. 23, 1240–1257.
Wu, J., Rogers, A., Albert, L.P., Ely, K., Prohaska, N., Wolfe, B.T., Oliveira Jr., R.C., Saleska, S.R., Serbin, S.P., 2019. Leaf reflectance spectroscopy captures variation in carboxylation capacity across species, canopy environment and leaf age in lowland moist tropical forests. New Phytol. 224, 663–674.
Wu, J., Serbin, S.P., Ely, K.S., Wolfe, B.T., Dickman, L.T., Grossiord, C., Michaletz, S.T., Collins, A.D., Detto, M., McDowell, N.G., 2020. The response of stomatal conductance to seasonal drought in tropical forests. Glob. Chang. Biol. 26, 823–839.
Xia, J., Niu, S., Ciais, P., Janssens, I.A., Chen, J., Ammann, C., Arain, A., Blanken, P.D., Cescatti, A., Bonal, D., 2015. Joint control of terrestrial gross primary productivity by plant phenology and physiology. Proc. Natl. Acad. Sci. 112, 2788–2793.
Xie, J., Wang, Z., Li, Y., 2022. Stomatal opening ratio mediates trait coordinating network adaptation to environmental gradients. New Phytol. 235, 907–922.
Xu, S., Yu, Z., Zhang, K., Ji, X., Yang, C., Sudicky, E.A., 2018. Simulating canopy conductance of the Haloxylon ammodendron shrubland in an arid inland river basin of Northwest China. Agric. For. Meteorol. 249, 22–34.
Yan, Z., Guo, Z., Serbin, S.P., Song, G., Zhao, Y., Chen, Y., Wu, S., Wang, J., Wang, X., Li, J., 2021. Spectroscopy outperforms leaf trait relationships for predicting photosynthetic capacity across different forest types. New Phytol. 232, 134–147.
Yan, H., Deng, S., Zhang, C., Wang, G., Zhao, S., Li, M., Liang, S., Jiang, J., Zhou, Y., 2023. Determination of energy partition of a cucumber grown Venlo-type greenhouse in Southeast China. Agric. Water Manag. 276, 108047.
Yang, X., Tang, J., Mustard, J.F., 2014. Beyond leaf color: comparing camera-based phenological metrics with leaf biochemical, biophysical, and spectral properties throughout the growing season of a temperate deciduous forest. J. Geophys. Res. Biogeosci. 119, 181–191.
Yang, X., Tang, J., Mustard, J.F., Wu, J., Zhao, K., Serbin, S., Lee, J.E., 2016. Seasonal variability of multiple leaf traits captured by leaf spectroscopy at two temperate deciduous forests. Remote Sens. Environ. 179, 1–12. https://doi.org/10.1016/j.rse.2016.03.026.
Yang, M., He, J., Sun, Z., Li, Q., Cai, J., Zhou, Q., Wollenweber, B., Jiang, D., Wang, X., 2023. Drought priming mechanisms in wheat elucidated by in-situ determination of dynamic stomatal behavior. Front. Plant Sci. 14, 1138494.
Zarco-Tejada, P.J., González-Dugo, V., Williams, L.E., Suárez, L., Berni, J.A.J., Goldhamer, D., Fereres, E., 2013. A PRI-based water stress index combining structural and chlorophyll effects: assessment using diurnal narrow-band airborne imagery and the CWSI thermal index. Remote Sens. Environ. 138, 38–50. https://doi.org/10.1016/J.RSE.2013.07.024.
Zelitch, I., 1961. Biochemical control of stomatal opening in leaves. Proc. Natl. Acad. Sci. 47, 1423–1433.
Zhang, Y., Wu, J., Wang, A., 2022. Comparison of various approaches for estimating leaf water content and stomatal conductance in different plant species using hyperspectral data. Ecol. Indic. 142, 109279 https://doi.org/10.1016/j.ecolind.2022.109278.